Non-invasive Measurement of Blood Components
Sensors for an In-Vivo Haemoglobin Measurement

J. Kraitl, D. Klinger, D. Fricke, U. Timm, and H. Ewald

University of Rostock,
Rostock, Germany

Abstract. This paper reports about fundamentals, simulations and measurements of optical absorption characteristics of whole blood and human tissues. A sensor system to measure blood components as haemoglobin is presented and corresponding results of in-vitro and in-vivo measurements. As basic technology NIR-spectroscopy and Photoplethysmography (PPG) is used for these non-invasive optical measurements. The characteristic absorption coefficient of blood in the visible and NIR region is well known and is mainly influenced by the different haemoglobin derivates. This fact is used to calculate the optical absorbability characteristics of blood which is yielding information about blood components as arterial oxygen saturation (SpO2), haemoglobin (Hb), carboxy-haemoglobin (CoHb) and met-haemoglobin. The measured PPG time signals and the ratio between the peak to peak pulse amplitudes are used for a calculation of these parameters. Haemoglobin is the main component of red blood cells. The primary function of Haemoglobin is the transport of oxygen from the lungs to the tissue and carbon dioxide back to the lungs. The Haemoglobin concentration in human blood is an important parameter in evaluating the physiological status of an individual and an essential parameter in every blood count. In currently standards, invasive methods are used to measure the Haemoglobin concentration, whereby blood is taken from the patient and subsequently analysed. Apart from the discomfort of drawing blood samples, an added disadvantage of this method is the delay between the blood collection and its analysis, which does not allow real time patient monitoring in critical situations. A non-invasive method allows pain free continuous on-line patient monitoring with minimum risk of infection and facilitates real time data monitoring allowing immediate clinical reaction to the measured data. The newly developed optical sensor systems uses up to five wavelengths in the range of 600 nm to 1400 nm for a measurement of the haemoglobin concentration, oxygen saturation and pulse. This non-invasive multi-spectral measurement method was tested with prototype-devices based on radiation of monochromatic light emitted by laser diodes and by using light emitting diodes (LED) through an area of skin on the finger. The sensors assembled in this investigation are fully integrated into wearable finger clips.

S.C. Mukhopadhyay et al. (Eds.): Advancement in Sensing Technology, SSMI 1, pp. 237–262.
springerlink.com

1 Introduction

Since the near infrared light was found to penetrate a great depth into biological tissues, near infrared spectroscopy has been developed into a non-invasive method for biomedical sensing and clinical diagnosis [1][2]. Oximetry is well known as typical example of a near-infrared application in clinic and can be used to non-invasive measure the oxygen saturation of human blood in-vivo [2]. The Haemoglobin concentration in human blood is also an important parameter to evaluate the physiological condition and the capability of oxygen transportation in blood. With this information anaemia (a low haemoglobin level) and polycythaemia vera (a high haemoglobin level) can be diagnosed and monitored. It is also possible to observe imminent postoperative bleedings and autologous retransfusions. Currently, invasive methods are used to measure the Haemoglobin concentration. For this purpose blood is taken and analysed. A disadvantage of this method is the delay between the blood collection and its analysis, which does not permit real-time patient monitoring in critical situations. A non-invasive method allows pain free online patient monitoring with minimum risk of infection and facilitates real time data monitoring allowing immediate clinical reaction to the measured data. It is well known that pulsatile changes of blood volume in tissue can be observed by measuring the transmission or reflection of light through it. This diagnostic method is called Photoplethysmography (PPG). The newly developed optical sensors system uses up to five wavelengths in the range of 600nm to 1400nm for the measurement of the haemoglobin concentration, oxygen saturation and pulse. For in-vitro tests and measurements a hemodynamic blood flow model has been developed which allows spectrometer measurements and the validation of the new sensors. A study to measure hypoxia showed that the sensitivity of the systems for measurement of SpO2 levels was accurate. In clinical measurements the ability to measure the haemoglobin content of blood in-vivo were proved and demonstrated.

2 Theoretical Aspects of HB-Measurements

The absorption and scattering of whole blood in the visible and near infrared range is dominated by the red blood cells, the different haemoglobin derivates and the blood plasma that consists mainly of water [3][4]. From the physiological point of view, the human skin and finger-tissue is particularly heterogeneous and therefore optically complicated, as shown in Figure 1. The radiation transport equation (1) can be regarded as the mathematical basis of tissue optics for the description of light-tissue interaction and the related phenomena [5][6].

$$\left(\frac{1}{c_n}\frac{\partial}{\partial t}+\vec{s}\tilde{N}\right)L(\vec{r},\vec{s},t)=-(\mu_a+\mu_s)L(\vec{r},\vec{s},t)+\mu_s\int_{4\pi}P(\vec{s},\vec{s}')L(\vec{r},\vec{s}',t)d\Omega'+Q(\vec{r},\vec{s},t) \qquad (1)$$

With $L(\vec{r},\vec{s},t)$ Radiance intensity of light at position $\vec{r}$ in direction $\vec{s}$ at time t

$c_n = \frac{c_0}{n}$	Velocity of light in tissue with index-of-refraction n
$(\vec{s},\vec{s}')$	Unit vector direction $\vec{s}$ and scattered direction $\vec{s}'$
$d\Omega' = \sin\upsilon'\partial\upsilon'\partial\varphi'$	Element of solid angle
$S(\vec{r},t)$	Energy intensity of the light source
$Q(\vec{r},\vec{s},t) = \frac{\partial S(\vec{r},t)}{\partial\Omega}$	Source term

Description of light-tissue interactions using the transport theory requires first to solve Eq.1. Because of difficulties to obtain exact solutions for biological tissue, several approximations have been made for the representations of $P(\vec{s},\vec{s}')$ and $L(\vec{r},\vec{s},t)$.

The pulsatile optical signal which is caused by the arterial blood flow in tissue [7] was detected and normalized with the non-pulsatile optical signal. This is necessary to eliminate the influence of the optical property changes of the venous blood and the bloodless tissue, and even the difference of tissue optical properties among patients (Figure 1).

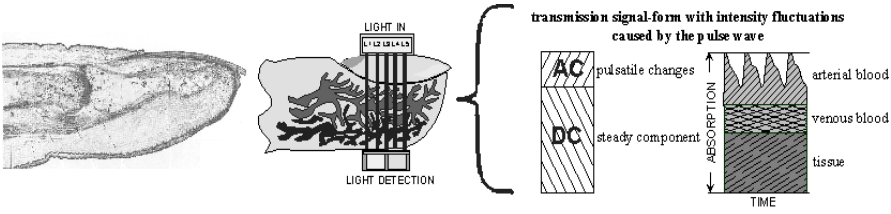

Fig. 1. Human fingertip [8] and principle of measurement

Beside the measurements of oxygenated (HbO_2) and reduced haemoglobin (HHb) for the calculation of oxygen saturation in the arterial blood (SpO_2), the noninvasive measurement of the haemoglobin concentration is a main objective of our application. Up to day the measurement of the haemoglobin concentration in blood needs an invasive method in clinical practice. The absorption and scattering of blood is influenced mainly by the total haemoglobin concentration and the amount of red blood cells (RBC's) as typical scatters. The light scattering behavior of biological tissue is a function of many variables such as the in-homogeneities in the refractive index as a result of the presence of blood vessels, blood cells, cell membranes and collagen structures within the tissue, which cause light scattering, i.e. change of the direction of photon propagation. The absorption-coefficient μ_a (in mm^{-1}), the scattering-coefficient μ_s (in mm^{-1}) and the so called phase-function $P(\vec{s},\vec{s}')$ are parameters necessary for the calculation of optical properties in turbid mediums like blood. The phase-function describes the probability of scattering for a photon traveling in direction $\vec{s}$ to be refracted in

direction $\vec{s}'$. Mathematical calculations can be simplified by using the anisotropy-factor $g = E(\cos(\vec{s}, \vec{s}'))$ instead of the phase-function and the reduced scattering-coefficient $\mu'_s = \mu_s(1- g)$ instead of the scattering-coefficient. To take the influence of light scattering into account, we assume that the measuring volume is composed of tissue (v^{Tissue} tissue volume, μ_a^{Tissue}, $\mu'_s{}^{Tissue}$ absorption and scattering coefficient tissue), arterial blood (v^{art} arterial blood volume, μ_a^{art}, $\mu'_s{}^{art}$ absorption and reduced scattering coefficient arterial blood), and venous blood (v^{ven} venous blood volume, μ_a^{ven}, $\mu'_s{}^{ven}$ absorption and reduced scattering coefficient venous blood). The model assumes further that the measuring volume can be considered as a homogeneous distribution of scatters and absorbers of the components mentioned [9]. Therefore, the Equations (2) to (6) are given in the following form for a human finger:

$$\mu_a^{Finger}(\lambda) = v^{artBlood}\mu_a^{artBlood}(\lambda) + v^{venBlood}\mu_a^{venBlood}(\lambda) + [1-(v^{artBlood} + v^{venBlood})]\mu_a^{Tissue}(\lambda) \quad (2)$$

$$\mu_a^{artBlood}(\lambda) = HSaO_2\mu_a^{HbO_2}(\lambda) + H(1-SaO_2)\mu_a^{HHb}(\lambda) + (1-H)\mu_a^{Plasma}(\lambda) \quad (3)$$

$$\mu_a^{venBlood}(\lambda) = HSvO_2\mu_a^{HbO_2}(\lambda) + H(1-SvO_2)\mu_a^{HHb}(\lambda) + (1-H)\mu_a^{Plasma}(\lambda) \quad (4)$$

and

$$\mu_s'^{Finger}(\lambda) = v^{Blood}\mu_s'^{Blood}(\lambda) + v^{Tissue}\mu_s'^{Tissue}(\lambda) \quad (5)$$

$$\mu_s'^{artBlood}(\lambda) = \mu_s'^{venBlood}(\lambda) = \mu_s'^{Blood}(\lambda) = f(H)\mu_s'^{Hb}(\lambda) \quad (6)$$

with H [0…1] = haematocrit (volume of red blood cells in whole blood)
v [0…1] = normalized volume

Our measurement method evaluates the PPG signal waveforms of peaks, troughs, steady averages, and pulsatile averages caused by the arterial blood volume shift $\Delta v(t)$ in the finger tissue [10]. With the assumption that $v^{artBlood} = v^{artBlood}(t)$ and $\Delta\mu_a = \Delta v\mu_a^{artBlood}$, follows Equation (7).

$$R = \frac{\Delta I}{I} = \frac{I(t+\Delta t) - I(t)}{I(t)} \approx \frac{\Delta\mu_a(\lambda)}{I}\frac{dI}{dt} = -\Delta\mu_a(\lambda)r \quad (7)$$

I = Intensity of light after interaction with the tissue

A multi-wavelength measurement with λ_k ($k = 1...K$) results in the following Equation:

$$(R_1, \cdots, R_K)^T = A(x_1, x_2, x_3)^T \quad (8)$$

with $(x_1, x_2, x_3) = \Delta vr(HSaO_2, H(1-SaO_2), 1-H)$ and $A = \begin{pmatrix} \mu_{a,1}^{HbO_2} & \mu_{a,1}^{HHb} & \mu_{a,1}^{Plasma} \\ \vdots & \vdots & \vdots \\ \mu_{a,K}^{HbO_2} & \mu_{a,K}^{HHb} & \mu_{a,K}^{Plasma} \end{pmatrix}$

With the mathematical model described before the measured PPG signals has been qualitatively analyzed by calculation of R_K-factors for each wavelength. But finally caused by the overwhelming nonlinear effects of tissue scattering a calibration of the PPG measurements has to be derived empirically by intensive statistical regression of the measurements obtained from volunteers and a hemodynamic blood tube model [10].

3 Simulation and Phantom-Models

3.1 Simulations of Tissue

Virtual modeling of turbid media, like biological tissue, and the description of photon transport in this media can lead to a better understanding of photonic processes and enables the effective development and optimization of optical systems.

In contrast to the analytical description of light-tissue-interaction with the already described radiation transport equation (1) a numerical method called Monte Carlo simulation or Monte Carlo ray tracing, provides considerable advantages like greater flexibility during model development and higher accuracy of the results [5][11]. Due to the stochastic nature of this method, the accuracy depends on the number of samples and thus on the number of simulated photons. Therefore the efficiency of this method has been improved in the last years by fast development of high-performance computational resources at an affordable price.

With the Monte-Carlo simulation (MC) it is possible to trace photons step by step through a turbid medium. A large quantity of the traced photons with their resulting paths in the medium results in a realistic mapping of the propagation of light in the target tissue. The medium itself is described by the optical parameters scattering coefficient μ_s, absorption coefficient μ_a, the anisotropy coefficient g and the index of refraction n. The tracing process of the photons can be described by few steps [12][13]. In a first step the photon flux is defined and the start position of the photon is assigned by its cartesian coordinates. The photon moves towards the direction of the tissue and hits the first surface. Due to the difference in the refractive index, only a certain amount of flux is transmitted through the surface which is described by the Fresnel's equations [14]. A further step describes the path length of the photon between two events like absorption and scattering. This path length must be chosen carefully in order to guarantee realistic photon paths on the one hand and to avoid an unnecessary reduction of the simulation speed on the other hand. This path length is randomly sampled by an exponential distribution which depends on absorption coefficient μ_a and scattering coefficient μ_s, however the mean free path length of the photon-tissue interaction is given by $1/(\mu_s+\mu_a)$. After moving the photon the described distance a decision is made for absorption, scattering and the new scattering direction. In the case of absorption the current photon energy E_{photon} is reduced by $\Delta E_{photon}=E_{photon}*\mu_a/(\mu_s+\mu_a)$.

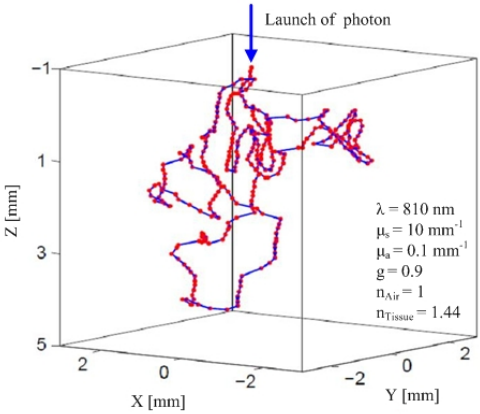

Fig. 2. Single photon path from Monte Carlo simulation

Dots mark the points of scattering and absorption events during the ray trace. Lines show the distributed free path length of the photon between the scattering and absorption events.

The Henyey-Greenstein phase function describes the probability of the polar deflection angle after each scattering event. The event depends on anisotropy coefficient g, which is equal to the mean cosine of scattering angle and variates between forward scattering g=1, isotropic scattering g=0 and back scattering g=-1. The tracing of the photon ends by total absorption on a certain layer or detector or by reaching a predefined cut-off-energy. In this case a new photon trace is started. In conclusion the relationship between absorption, scattering and mean free path length are displayed as a single photon path in Figure 2.

The simulations of light-tissue interactions were performed with the optic software ASAP® (Breault Research). ASAP® includes functions for simulations of geometric- and physical-optical properties and delivers complete 3D-models of optical and mechanical systems. In addition the Monte-Carlo simulation is already implemented in the software.

Besides the simulation of multi-layered tissue models, ASAP® in our case is used to simulate cuvettes and blood transporting tubing's of our blood flow model. The results of the simulations provide important information such as optical path lengths, penetration depths and internal distributions of the energy in the target tissues. Furthermore the simulations supplement the analysis of real measurements.

As already mentioned above, the basic model for simulations consists of a virtual volume which is described by his optical properties. Basically it's possible to model arbitrary complex systems. In the case of human tissue excessive complex models are counterproductive under certain circumstances for at leas two reasons. Wavelength dependent optical parameters for tissue sub structures as hair follicles, sweat glands and pacinian corpuscles are limited available. These sub systems have only small contribution to the whole system and can be easier described in the context of a functional layer, like tissue layers. Consequently simple models consists

only of one single tissue layer where all specific different optical properties are reduced to only one u_s, u_a, g and n. More complex systems like the following in figure 3 and figure 4 consist of up to five functional isolated tissue layers.

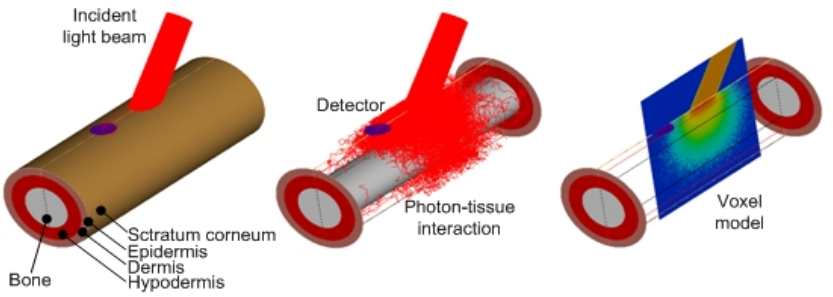

Fig. 3. Simulation of finger-model with ASAP®

The finger-model consists of the main layers stratum corneum, epidermis, dermis, hypodermis and bone. The light is obliquely incident on the stratum corneum surface and penetrates the first layer. Inside the finger model the photons are scattered and absorbed, according to the predefined optical tissue parameters μ_a, μ_s, g and the refraction index n. A Voxel-model allows the visualization of the irradiance.

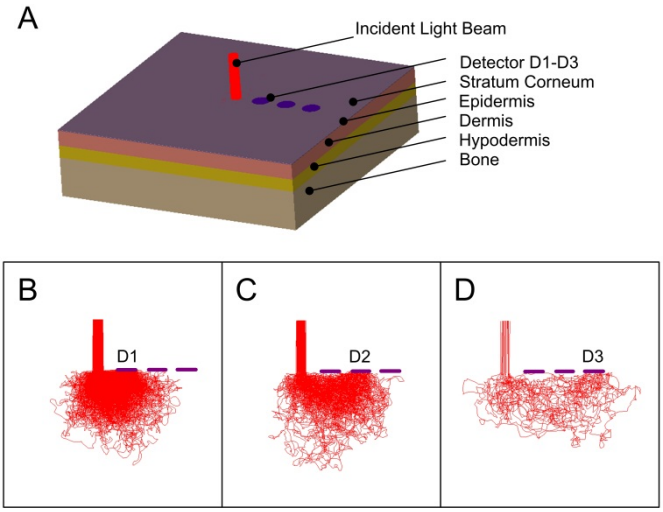

Fig. 4. Simulation of five layer tissue model with ASAP® **A:** Five layer tissue model consisting of the layers stratum corneum, epidermis, dermis, hypodermis and bone. Three detectors are positioned in different radial distances from the incident light beam. **B, C and D:** Lateral view of the tissue model from A with Detectors D1-D3. Displayed are only the rays corresponding to the detector.

The tissue model is implemented as a section of a human finger. The first layer in this model represents the stratum corneum. This outer layer, about 20 µm thin, consists of dead cells and forms a barrier to protect underlying tissue from environmental influences. The epidermis is the subsequent layer, about 80 µm thin, and consists of living cells. It regulates the amount of water released from the tissue and contains high amounts of light absorbing melanin pigments. Below this layer is the dermis located. It is mainly connective tissue based on collagen fibers with continuous blood perfusion. Therefore the light scattering and absorption in this layer is dominated by haemoglobin. The dermal scattering results primarily from the collagen fibers. The next layer is named hypodermis and is used basically for fat storage. The center of the model consists of bone. In the present case a section of the intermediate phalanges is modeled. For plethysmography like simulations a model of the distal phalanges is required.

3.2 Integrating-Sphere Measurement System

For simulations of biological tissues wavelength dependent optical parameters especially the scattering- and absorptions coefficients are required as inputs. Those parameters can be partially gained from various publications and literature [4][15][16][17][18]. Due to the variation of composition of biological tissues it should be noted that there are also deviations in the published data. Optical parameters for tissues containing different scenarios for quantitative compositions, like haemoglobin (Hb), carboxy-haemoglobin (CoHb) and arterial oxygen saturation (SpO2), are rarely incomplete or not available.

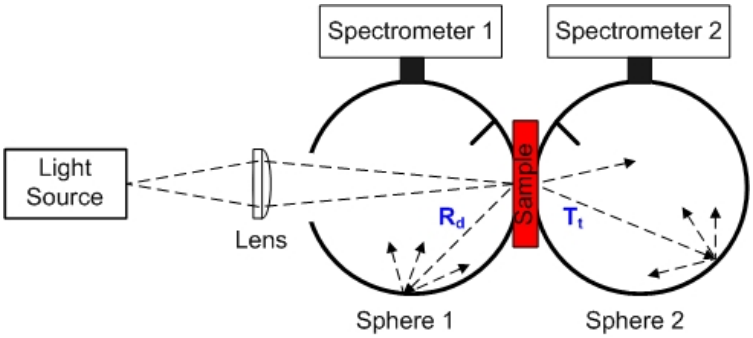

Fig. 5. Double integrating sphere system

The system consists of two integrating spheres with the blood sample between. The light of a halogen wide band light source is focused on the sample. Two fiber coupled spectrometers detecting the reflected and transmitted light. The data are acquired and post processed. The inverse adding-doubling method is used to calculate the scattering and absorption coefficients out of R_d and T_t.

The measurements of optical properties of tissue are made in the classical manner with an integrating sphere setup. This measuring system illuminates a tissue sample with light and detects the reflected and transmitted parts of light separately. In a further step this data are used to calculate the absorption and scattering μ_a and μ_s. For the integration of the reflected and transmitted light R_d and T_t, integrating spheres are used. Those hollow spheres have several input and output ports and a high reflection coating on the inner side. The coating material is adjusted to the wavelength range for the measurements and can be divided into barium sulfate ($BaSO_4$) and polytetrafluoroethylene (PTFE) for application in the visible and near-infrared region and gold coatings for the measurements in the near and far-infrared spectral region.

The integration of the light in the sphere is achieved by a high number of reflections. Basically it is possible to carry out the measurement of R_d and T_t with one sphere. A system based on two spheres has the advantage to measure R_d and T_t simultaneously without changing the setup and therefore reduces measurement artifacts due to undesired position changes of the sample. Therefore a double sphere setup also reduces the measuring time.

The detection of the integrated light depends on the used light source. Narrow band light sources allow the detection with photomultipliers or photodiodes and hence connect the illumination with high spectral irradiance and sensitive detection. The use of lock-in technique can increase the signal-to-noise ratio additionally. In order to acquire optical properties over a wide spectral range at once, light sources like halogen lamps in combination with spectrometers are used. Therefore optical parameters from visible or near-infrared spectrum can be recorded in a single step.

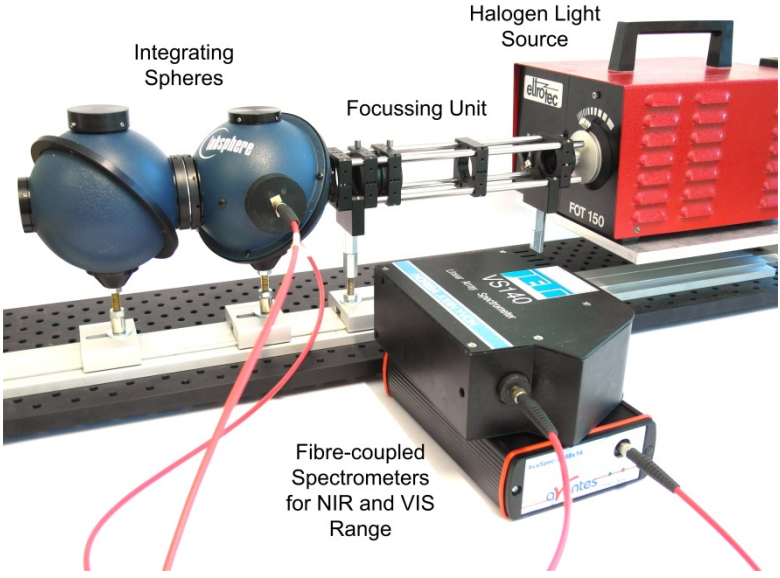

Fig. 6. Double integrating sphere setup

The labor measurement setup consists of two 4" integrating spheres (SphereOptics GmbH) with a Spectraflect® coating which is optimized for visible and near-infrared region. As a light source a modified 150W FOT150 halogen lamp (Eltrotec) is used. The light is focused over a system of pinholes and a plano-convex lens on the sample. The sample itself is fixed in a cuvette and placed between the spheres. Depending on the wavelength range and the sample, the thickness of the cuvettes ranges between 0.5 mm and 2 mm. Saline is used to reduce the mismatch of index of refraction between tissue and cuvette.

The integrated fraction of R_d and T_t is guided from the sphere ports through a fibre to the fibre coupled spectrometers. The spectrometer Avaspec covers a wavelength range from 370 nm - 920 nm with an optical resolution of 0.5 nm, while the VS 140 NIR spectrometer (HORIBA Scientific) covers a wavelength range from 800 m - 1700nm with an optical resolution of 7 nm. A diffuse reflectance standard (Spectralon®, LabSphere) is used for the calibration of the setup.

The calculation of the absorption and scattering coefficients μ_a and μ_s out of R_d and T_t is performed by the iterative algorithm named inverse adding-doubling method (IAD) [6]. This numerical method is based on the solution of the radiation transport equation for plane-parallel layers and considers the aspect of the inverse scattering problem. In a first step of the solution, the optical parameters for a thin sample layer are estimated. Through the solution of the one dimensional radiation transport equation R_d and T_t are calculated and compared with the measured values. In the case they are not corresponding, μ_a and μ_s varies until they match. In a second step the sample thickness is doubled and the procedure from step number one is repeated until the final sample thickness is reached. The „adding" involves in the calculation of μ_a and μ_s inhomogeneous media with internal reflections between the different tissue layers due to differences in the index of refraction.

Double integrating spheres combined with an inverse adding–doubling algorithm produce accurate values of μ_a and μ_s. Furthermore the presented setup can be expanded to measure also the anisotropy g if the collimated transmission is measured at some distance from the sample through a hole in the second sphere.

3.3 Optical Tissue Phantoms

The development and calibration of optical plethysmography systems require references with stable scattering and absorption properties [19]. The transmission and reflection measurements with human tissues show, in contrast to the required standard, considerable volatility in time. There are multiple reasons for this: thickness changes because of volume changes in the arteries, hydration status, difference in chromospheres concentrations, and oxygenation of the blood, temperature and perfusion status. The required calibration standards, named tissue phantoms, imitate the optical properties of human tissue and are characterized, contrary to human tissue, by time constant absorption and scattering and guarantee therefore repeatable measurements.

For the design of tissue phantoms it is recommended to look at the scattering and absorption separately. The scattering in human tissue is caused by mismatch of index of refraction between nuclei of the cells, cell organelles and the cell walls. This scattering can be reproduced by isolated microspheres with given diameters and index of refraction [20]. The absorption in tissue phantoms is realised by dyes, ideally with no scattering properties [21]. Because most of the dyes absorb in a narrow-band, the peak wavelength must be adjusted to the desired measurement wavelength. The carrier material for the dye and scattering particles has also ideally no absorption and scattering properties.

Tissue phantoms can be basically subdivide in tow categories: liquid phantoms and solid phantoms [22]. Liquid phantoms, like the fat emulsion infusion Intralipid, have the advantage that the detector can be moved also inside the phantom. The main disadvantage of liquid phantoms is the missing possibility to create complex shapes like multi layer systems. Furthermore the additives in the liquid can deposit over the time and change therefore the optical properties. However solid state phantoms are more complex in the processing but keep the optical properties stable over time.

A typical base material for solid state phantoms is epoxy resin or silicone gel. Due to the diameter within the lower µm range and similar refractive index to cellular structures, quartz microspheres are the ideal material choice for high forward anisotropic scattering imitations. Another, much cheaper scattering material is titanium dioxide but the nano-sized particles of this powder reducing the forward scattering characteristic. Common dyes for phantoms in the visible spectral range are Trypan blue and India ink. Pro-Jet 900 NP [23] is used for phantoms in the near-infrared region.

The manufacturing process of solid phantom can be described by the following steps. In the first stage a suitable quantity of scattering particles and absorbing dyes is mixed properly with the base material epoxy resin and placed in an ultrasonic bath for an ideal seperation of the particles. In a further step the hardener is added in a prescribed ratio and the suspension is mixed again. The bubbles in the liquid can be eliminated effective by placing the suspension in a vacuum chamber. In the last step the suspension is cast into shape and hardens at room temperature or elevated temperature.

The measurement of the optical properties of the finished phantom is performed with the already described integrating sphere system.

4 Haemodynamic Blood Flow Model

An artificial blood flow model (BFM) based on the human circulatory system was developed to allow a controlled variation of the blood parameter as total haemoglobin concentration (ctHb), oxyhaemoglobin (O2Hb), carboxyhaemoglobin (COHb) and methaemoglobin (MetHb). For this reason the optical properties of the blood were observed continuously by spectrometer measurements to determine the absorption, transmission and scattering properties of human whole blood in a wavelength range from 400 to 1700 nm and to test new noninvasive measurement systems.

4.1 Structure of the Model

For all measurements donor erythrocyte concentrates were used. The concentration of haemoglobin was changed by adding fixed amounts of blood plasma to the erythrocyte concentrate. Blood circulation and predetermined oxygen state were adjusted with an extra-corporal circulation unit. The blood was gently stirred and kept flowing through the blood tubes and the specially designed cuvettes (for spectrometric measurements). The blood temperature was kept constant at 37 °C via a tube heating mechanism and a separate water circulation through the Oxygenator.

The following blood parameters were varied by using the blood flow model:

- total haemoglobin (ΔctHb)
- oxyhaemoglobin (ΔO_2Hb)
- carboxyhaemoglobin (ΔCOHb)
- deoxyhaemoglobin ((ΔHHb)
- temperature (ΔT)
- flowrate (ΔQ)
- kind of fumigation (N_2-CO, N_2, compressed air)
- flowrate of fumigation

The model enables a defined circulation of app. 250 ml of human blood. The peristaltic blood pump has a maximum rotation speed of 250 rpm (Q: 0 to 200 ml/min).

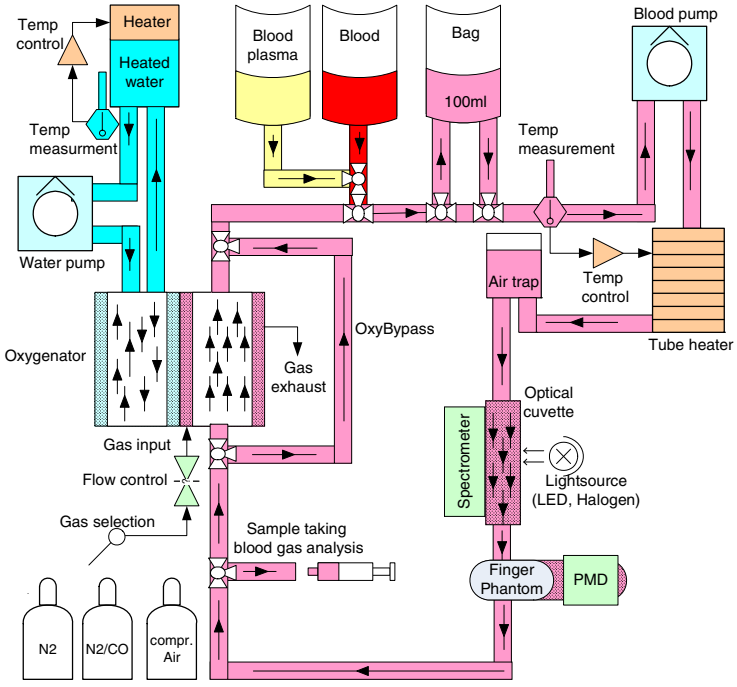

Fig. 7. Structure of the blood flow model

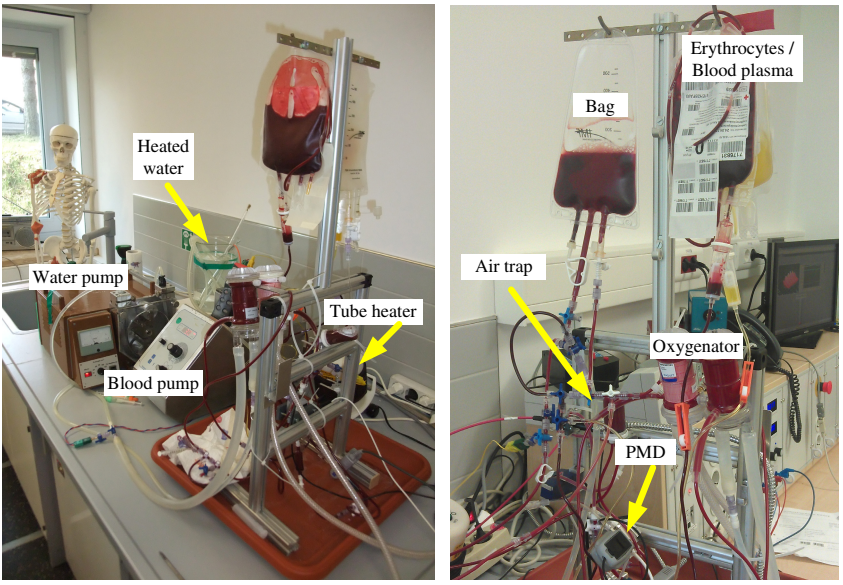

Fig. 8. Set up blood stream model

To avoid bubbles in the circuit an air trap was installed. To change the oxygen saturation a hollow fibre was used. Diverse gas molecules were transferred to the haemoglobin via the membrane surface. Nitrogen was used for desaturation and compressed air for oxygenation. The gas support enables flow rates of up to 5 l/min. The donated blood stored in blood banks was warmed up to 37°C before filled in the circulatory.

An additional bag in the bypass of the oxygenator were used to stabilize the system after changing the blood parameters so that defined conditions of the system could be hold for a while. Next to the optical cuvettes is port located for the extraction of blood samples for reference measurements with external devices as a BGA.

4.2 Optical Measurement System

To determine the optical properties of the blood components two grid spectrometer were used. With these spectrometers it is feasible to cover an area from 370nm to 1700 nm to obtain transmission data of whole blood for the comparison with literature data [10,24,25]

The blood mixture circulates in an artificial circuit with optical cuvettes. Different thicknesses of the cuvettes (0.5, 1, 2 and 3 mm) were realized to extend the dynamic area of the spectrometer. In figure 4 the first double layer cuvette is shown.

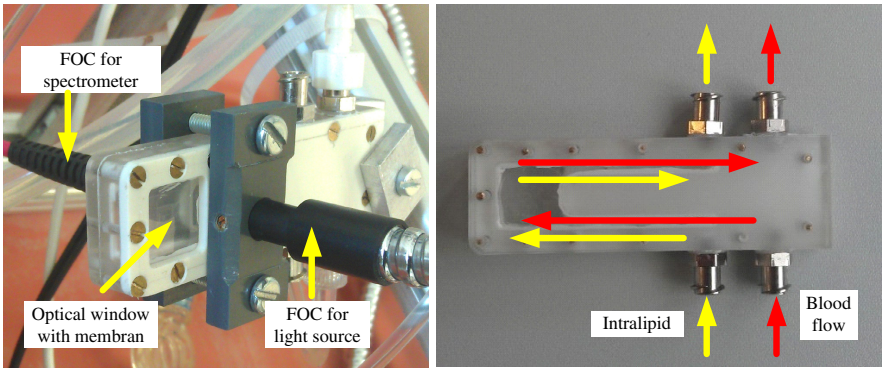

Fig. 9. Double layer optical cuvette (finger phantom) with membrane

This cuvette contains of two channels, one for the blood flow and one for intralipid to simulate human tissue. An optical window with a flexible membrane was used to generate PPG signals.

As light source different lamps where used, a wolfram halogen lamp with an interface to a fibre optical cable and a diameter of 6 mm. In the wavelength area below 700 nm an additional white LED power lamp (15W) was used. In opposite to the light sources the transmitted light was coupled in a 600 µm FOC with SMA interface which ends in a spectrometer.

4.3 Results

In first measurements the transmission spectra of water was determined to verify the measurement system and compare the results of the model with literature data [26].

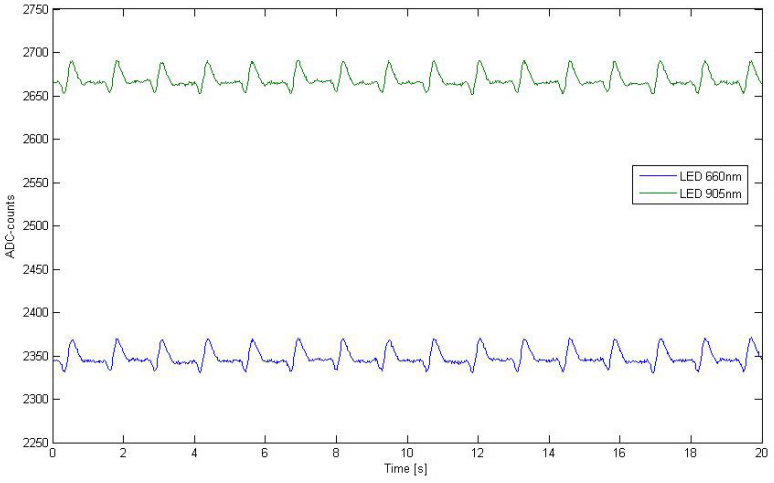

Fig. 10. Plethysmographical signals measured with the PMD

Figure 10 shows the plethysmographical signals of the finger phantom with blood and intralipid inside. The peristaltic blood pump was driven at 30 rpm (that corresponds to a heart rate of app. 60 bpm). The pressure of the blood pump was adjusted in a way to avoid a destruction of the erythrocytes (haemolysis).

Figure 11 shows the LED signals (660 nm, 905 nm) of the PMD on the finger phantom during the deoxygenation process in the blood flow model. The haemoglobin concentration was fixed at 5.3 mmol/l and proven by measurements with the blood gas analyzer (BGA). The tube heater and the additional water cycle maintain the blood temperature at app. 37°C.

For the complete oxygenation the compressed air was used to reach an oxygenation of 96 % O_2Hb. The deoxygenation was started with the pure nitrogen gas in periods of some minutes. The oxyhaemoglobin could be reduced to different levels and kept constant for a while to build up the system.

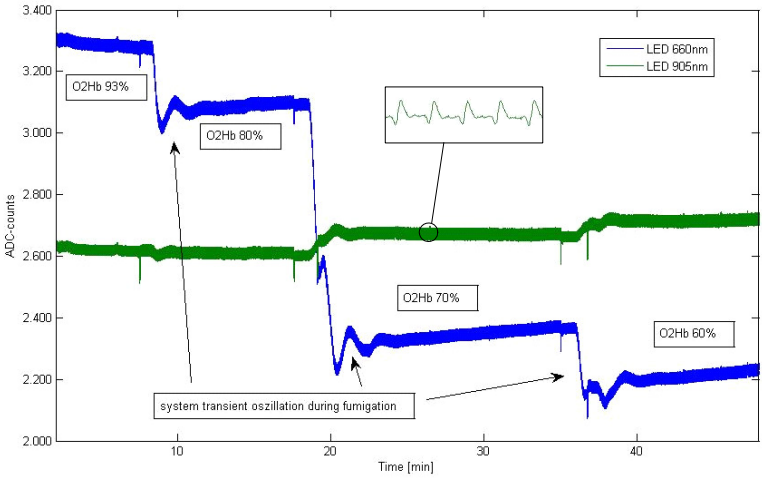

Fig. 11. PMD LED signals during deoxygenating in the blood model

The curves offer the measuring effect of deoxygenated blood by 660 nm and the contrary effect by 905 nm.

In figure 12 different O2Hb in the spectrum are displayed. In this diagram the oxyhaemoglobin values of 95%, 82% und 71 % are shown.

Figure 13 shows the absorption spectra of a blood solution with different COHb values (left) and MetHb values (right) through a 0.5 mm cuvette.

With the presented blood flow model different levels of total haemoglobin, oxyhaemoglobin, deoxyhaemoglobin, carboxyhaemoglobin and methaemoglobin could be realized. With the optical measurement system and the developed cuvettes the dynamic range of the spectrometer could be adapted to new measurement conditions.

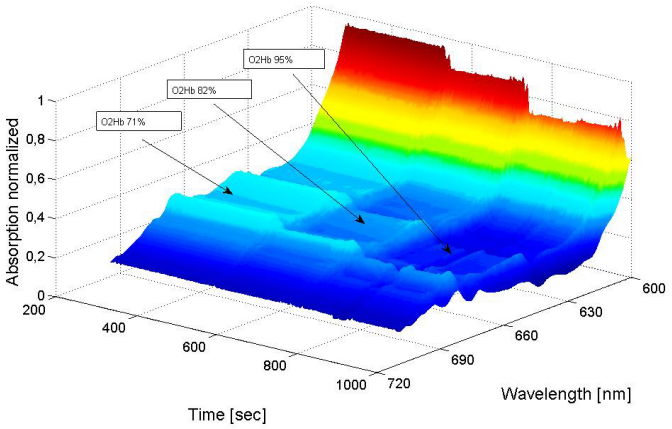

Fig. 12. Absorption spectrum blood on BFM

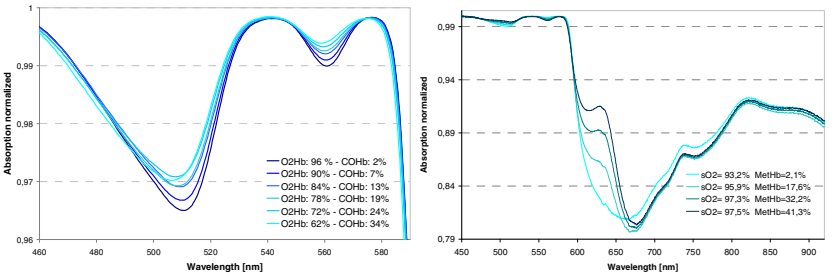

Fig. 13. Spectrum of different COHb and MetHb

First prototypes of non-invasive sensors were tested and PPG-signals could be generated, recorded and analysed on the model. Also calibration procedures for the prototypes are possible on the BFM.

5 Non-invasive HB-Measurement Method

The new developed non-invasive sensor systems allow a continuous measurement of the haemoglobin concentration, oxygen saturation and pulse which is based on a pulse-photometric measurement method. Thereby an area of skin on the fingertip is trans-illuminated by light which is emitted by Laser-diodes or LEDs in the range from 600nm - 1400nm. The objective of the photometric devices described here is the non-invasive continuous measurement of heart circulation patterns and light absorbent blood components in the blood of the human finger. The arteries contain more blood during the systolic phase of the heart than during the diastolic phase, due to an increased diameter of the arteries during the systolic phase. This effect occurs only in arteries but normally not in veins. For this reason the absorbance of light in tissues with arteries increases during systole because the

amount of haemoglobin (absorber) is higher and the light passes through a longer optical path length in the arteries. These intensity changes are the so called PPG-waves. The time varying part allows the differentiation between the absorbance due to venous blood and bloodless tissue (DC part) and that due to the pulsatile component of the total absorbance (AC part). Upon interaction with the tissue the transmitted light is detected non-invasively by photo diodes. Suitable wavelengths derived from measurements with the blood stream model were selected for the analyses of relative haemoglobin concentration change and SpO_2 measurement. During the measurement of haemoglobin the absorption should not depend on the oxygen saturation. The principle of measurement is based on the fact of a substantial absorption/transmission difference of light in red and near infrared region between oxygenated (HbO_2) and reduced haemoglobin (HHb) and blood plasma (optical mainly water). HHb is optically much denser to the red light (600 to 750 nm) than HbO_2, whereas the reverse is true in the near infrared region (900 to 1000 nm), even to a lesser degree. We selected suitable wavelengths to analyse the SpO_2 and relative haemoglobin concentration change for our application. Four of the five laser diodes of the newly developed laser based Photometric I device (PMD I) emits light in the range of wavelengths between 600 – 1000 nm (670, 808, 905 and 980 nm). This is the therapeutic window region, in which the blood absorption is dominated by the haemoglobin derivatives. An additionally 1300 nm laser diode is integrated, At this wavelength the absorption of water is dominant. For a calculation of haemoglobin, the wavelengths are chosen to suit the absorbance peaks of water in blood where the two components of blood have differing amounts of water (980 nm, 1310 nm). To find a value corresponding to an isosbestic point for absorbance of oxy-haemoglobin and deoxy-haemoglobin, a wavelength of 808 nm is chosen. A second relationship for the measurement and correction of oxygen saturation is calculated with the 670 nm (absorbance of deoxy-haemoglobin greatly exceeds the absorbance of oxy-haemoglobin) and 905 nm (absorbance of oxy-haemoglobin greatly exceeds the absorbance of deoxy-haemoglobin) transmission signals. Additionally we developed a LED based Photometric II device (PMD II) which operates three LEDs as optical light sources with center wavelengths of 670 nm, 810 nm and 1300 nm.

6 Measurement Devices

The Photometric I device PMD I (Figure 14) is basically a main box of electronic components, a light probe and a Laptop or PC for display and data storing [27]. The probe is attached to the patient's body usually the finger. Red to Near Infrared light is transmitted sequentially through the body tissue via fast –switching laser diodes and special driver electronics. The transmitted light is picked up with two suitably positioned photodiodes. Inside the measurement device the laser diodes are integrated together with the required control electronics. The main unit electronics consists of the components required for signal amplification, digitalization, and triggering of the laser diodes, which operate in a time-multiplex pulse mode. The sample frequency of the system is about 7 kHz. After mean value calculation and subtraction of the dark-current inside the main unit, the transfer of the five photocurrents is achieved with a sample rate of about 120 Hz each. The laser light is transmitted to a special optical transmission head by means of optical

fibers inside the sensor probe. Two Photo-detectors are also contained in the sensor head together with the required pre-amplifiers; the sensor signals detected here will be processed inside the measurement device.

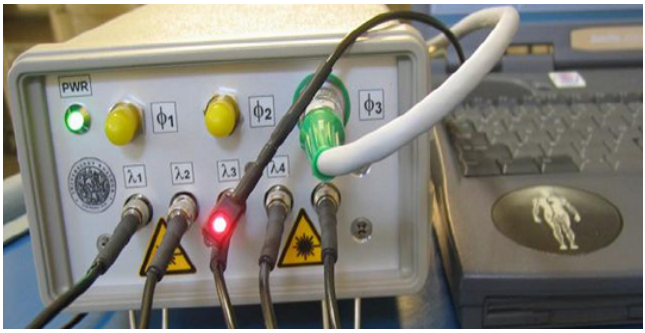

Fig. 14. PMD I front panel with fibre optics and transmission head

Figure 14 shows a photo of the PMD I device and the fiber optical sensor head used to transfer the laser light into the finger tissue. To detect the transmission signals of lasers 1 to 4 (670 nm to 980 nm) a Silicon Photodiode is used with a spectral sensitivity of 400 nm to 1150 nm. To detect the 1310 nm transmission signal an InGaAs-Photodiode is required with a spectral sensitivity of 1000 nm to 1700 nm. The application software is programmed in LabView (Figure 15).

Fig. 15. PMD I Software Frontpanel for Hb measurement

The second sensor system Photometric device II (PMD II) being developed consists of hardware modules including appropriate light sources and receivers, a microcontroller and a wireless interface [28]. Figure 16 shows a functional block diagram of the PMD II device.

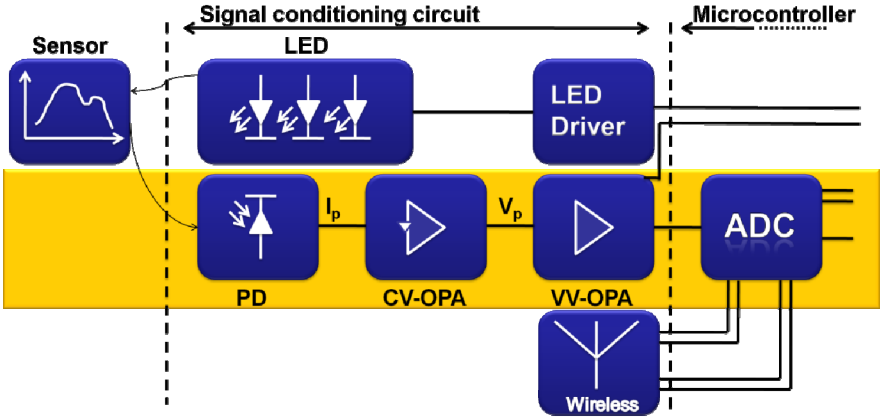

Fig. 16. PMD II: block diagram

The sensor system is low powered from a battery. A key component allows low power wireless operation, is the low power microcontroller MSP430F1611. This enables software controlled and time multiplexed operation of the light sources and receiver channels. The mean value is calculated and dark current subtracted in software, and the data is transmitted via serial USB or the wireless Bluetooth or ZigBee interface. The light sources, three LEDs, with centre wavelengths of 670nm, 810nm and 1300nm are installed in the upper part of the clip. The pulsed LED currents are controlled by the microcontroller, which allows a change of the light source intensity. To detect the transmission signals an Indium Gallium Arsenide/Indium-Phosphor photodiode was chosen. With a spectral range of 400nm-1700nm a measurement at all three used wavelengths is feasible. All components of the sensor system are chosen to guarantee low power consumption.

Fig. 17. High performance Hb-Sensor (PMD II) from Bluepoint Medical GmbH

Figure 17 shows the newly developed HB-Sensor OxyTrue Hb^{TM}. The prototype software runs on a touch screen PC.

Fig. 18. PMD II PC with Display and storage software

With the developed application software programmed in LabVIEW^{TM} it is possible to handle, analyze and store the data (Figure 18).

7 Application and Results with Prototypes

The PMD I and PMD II Prototype-devices was tested in-vitro with the blood stream model and in-vivo on volunteers and patients.

7.1 In-Vitro Results with the Prototypes

Figure 19 and Figure 20 show results measured with the PMD I and compared with the BGA reference values for two in-vitro measurements with the blood stream model. At first the oxygen level of the blood variants from 100% to 3% and the haemoglobin concentration remains constant at 88g/l. During the second measurement (Figure 20) the haemoglobin concentration was changed from 206 g/l to 50 g/l with a constant oxygen saturation of 97 %. Figure 19 shows that the measured and calculated coefficient for haemoglobin concentration was not affected by the different blood spectra for HHb and HbO_2. We found a non-linear relationship between the haemoglobin concentration and the calculated R coefficients measured with the PMD I. As expected, the oxygenation state of the blood was found to have no discernible effect on light attenuation at the 808 nm and 1310 nm wavelength, confirming that these wavelengths are isosbestic for HHb and HbO_2. After an empirically derived partial least-squares (PLS) calibration and statistical regression of the PMD I measurements the application is able to measure the Hb and sO_2 value in whole blood very well.

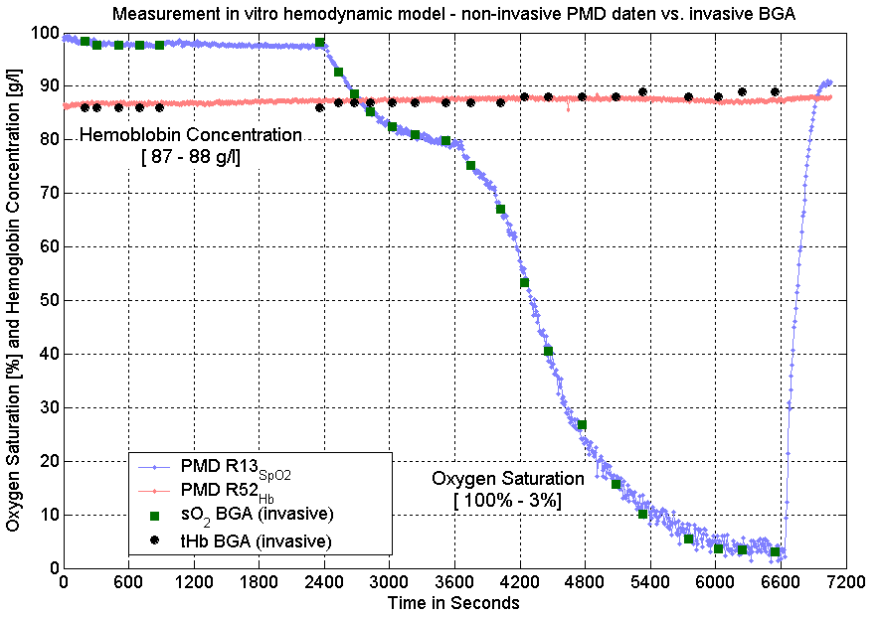

Fig. 19. Measurement of sO_2 and Hb with the PMD I through a blood tube of an in-vitro model

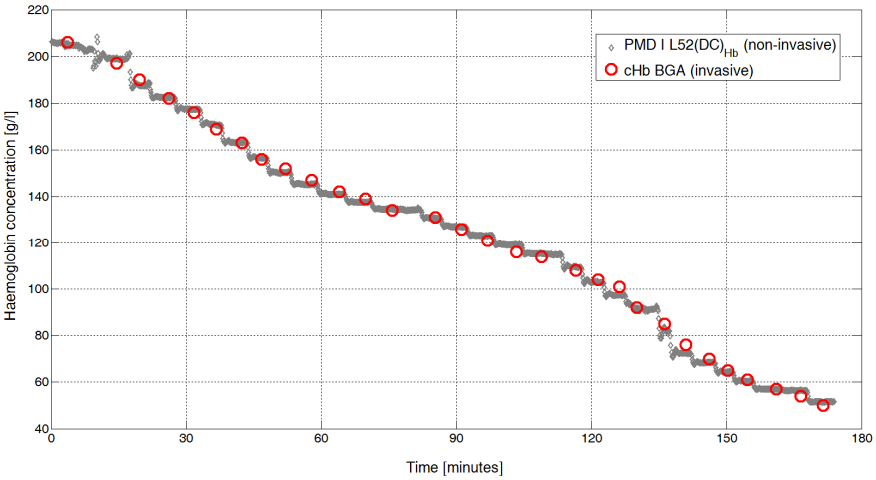

Fig. 20. Non-invasive measurement of HB (206g/l to 50g/l) with the PMD I in-vitro

7.2 In-Vivo Measurements

After a good correspondence between in-vitro experimental results with a blood tube system and our mathematic model, we used the PMD I to measure the arterial blood oxygenation and haemoglobin concentration for studies with healthy subjects. Previous measurements of the transmission signals of the five wavelengths had shown an apparent variation of the arterial pulse during in-vivo measurements. The signal quality was sufficient to analyze the signal components and to calculate relative attenuation coefficients of the arterial blood. With regard to the components at 1300 nm an evaluation of the relative portions of haemoglobin and water in the blood is feasible. The in-vivo measurement technique requires a pulse signal for the calculation of the relative attenuation coefficients. Vasoconstriction at the extremities can be a problem, as it decreases the signal amplitude, and therefore the signal to noise ratio. A small signal amplitude tends to give inaccurate results. The PMD sensors have therefore, a minimum signal amplitude below which no value for the calculated coefficient is displayed. The lower limit for the pulse amplitude with the 1300 nm laser or LED is in the order of 0.2% of the measured intensity. This may be a limitation when using the system on various patient groups (vascular disease, Raynaud's phenomenon, shock etc.). The non-invasive measurement method for haemoglobin and arterial oxygenic saturation described in this paper might be applicable for clinical applications where an invasive method is undesirable or inconvenient. One particular application could be the monitoring of patients vital signs in Critical Care Medicine or Anesthesia. Another application might be in the monitoring of patients who are undergoing surgery, were presumably the loss of blood during surgery would produce a change of haemoglobin concentration. It may also be a useful tool during dialysis sessions for the monitoring of haemodialysis patients with end stage renal failure. By using a dialyser (haemofilter) the patient has dialysat (prevailing water) distracted. This deferral means a fluid reduction for the patient during the ultra filtration. The change in blood volume involves a change of the haemoglobin status. It is necessary to compute a correction factor and the influence against deferrals in the arterial oxygen saturation for a photometric non-invasive measurement of haemoglobin. During a hypoxia-study the device sensitivity was validated for SpO_2. The pulsatile changes in the intensity observed with the PMD were caused by changes in arterial blood volume. It has thereby been assumed that the arterial blood volume fluctuations do not introduce pulsatile changes of the venous (and capillary blood) volume fraction. The PPG signal intensity of the 670nm and 905 nm wavelength from PMD I is used to compute the SpO_2 value. Figure 21 shows a measurement during a hypoxia study for one subject. The arterial oxygen saturation was reduced to about 75%. Thereby the recorded data of the photometric device PMD was compared with the data of a blood-gas-analysis BGA from the A. radialis (arterial oxygenic saturation - SpO_2 in percent). The results for 4 subjects showed a high sensitivity and high reproducibility for all measurements with the photometric device.

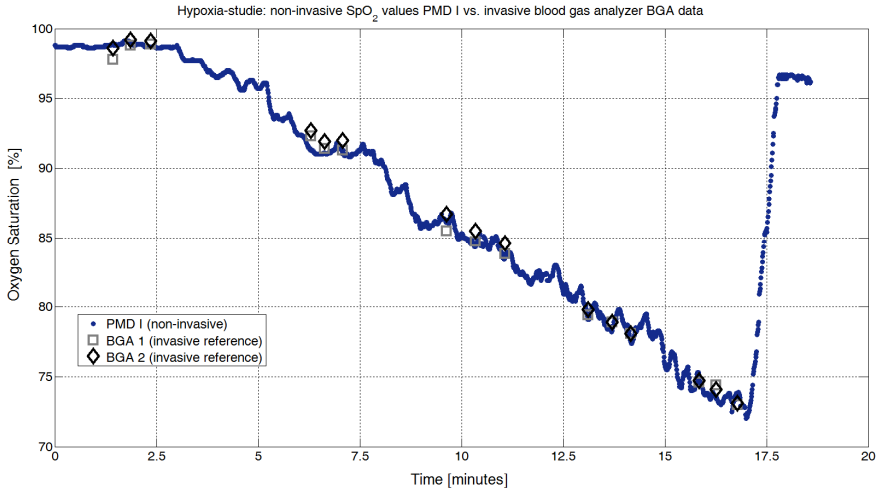

Fig. 21. SpO2 PMD I, compared with invasive BGA

A study with n=43 adult healthy male and female volunteers (range 19 - 60 years, 15 women and 28 men) was performed to test the ability of PMD I to measure the haemoglobin content non-invasive. The third or fourth finger of the left hand was connected with the PMD I sensor. The photometric measurements spanning 3 to 5 minutes for each subject and were stored using the PMD I system. After that the data was analyzed and the PMD I R_{Hb} coefficient was computed for each subject. A HemoCue™ haemoglobin device (HemoCue AB, Sweden) was used for invasive reference measurements. This system provides reliable quantitative haemoglobin results with the same performance as a large haematology analyser. A drop of capillary blood was taken from the same fingertip used for the photometric measurements for each volunteer, and analyzed with the HemoCue™ device. The Figure 22 shows the results of the non-invasive photometric measurements vs. the invasive measured haemoglobin values (131 measurements). In this study, we achieved good results with our application for a non-invasive haemoglobin determination. For this study the squared correlation coefficient is 0.918.

The example is too small to represent the variability in the population. Therefore the whole data set of 43 volunteers is not sufficient by itself to further evaluate the effects of patient-to-patient variation on the measurement method. The potential of this photometric method to measure the non-invasive haemoglobin in-vivo were proved with a good result. Future work will involve further clinical studies, which allows an extensive statistical analysis of these measurements.

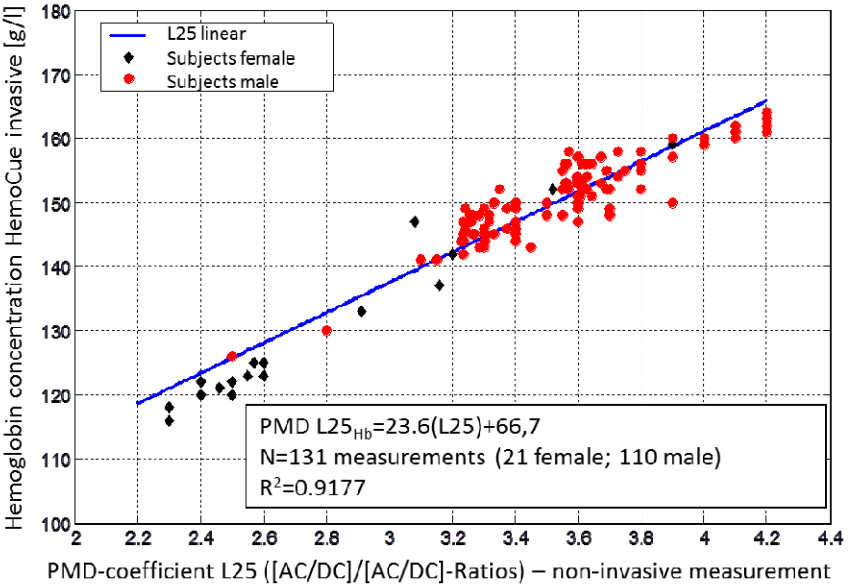

Fig. 22. Non-invasive PMD I HB coefficient vs. invasive HemoCue (R=0.95)

8 Conclusions

In this paper a multi-wavelength photometric measurement method that provides non-invasive in-vivo spectral measurements in human blood and tissue as well as the monitoring of heart circulation patterns has been described. A newly developed laser based PMD I and a LED based PMD II device has been introduced that is able to measure PPG-signals continuously at different wavelengths from 600 nm up to 1400 nm. The fact that the absorption-coefficients μ_a and scattering-coefficients μ_s for blood differ at difference wavelengths has been exploited and is used for calculation of the optical absorbability characteristics of human blood yielding information on the blood composition. A trial study to measure hypoxia showed that the sensitivity of the PMD I system for measurement of SpO2 levels was precise. In the first clinical measurements of the new measurement system, the potential to measure the haemoglobin content of blood in-vivo were proved and demonstrated. What could not be determined so fare in a first approach is a measurement with a large group of patients and volunteers. Future work will involve further clinical studies with this measurement method. A main aspect is the test of the optimized hardware system (PMD II) and a further evaluation of suitable statistical on-line analysis algorithms for the blood components. Future work in frame of the so called project PHOTOSENS includes the investigation and development of motion tolerant PPG measurement during low perfusion, the noninvasive measurement of carboxy-haemoglobin and the noninvasive determination of tissue dehydration.

Acknowledgment. This work was conducted within the framework of the project PHOTOSENS and has been funded with financial support from the Ministry of Economics, Labor and Tourism of the State Mecklenburg-Western Pomerania, Germany. A large part of this work was realized in close cooperation with our industrial partner bluepoint MEDICAL GmbH, Selmsdorf in Germany.

References

[1] Wukitsch, M.W., Petterson, M.T., Tobler, D.R., Prologe, J.A.: pulse oximetry: analysis of theory, technology, and practice. J. Clin. Monit. 4, 290–301 (1988)
[2] Ahrens, T., Rutherford, K.: Essentials of Oxygenation: Implication for Clinical Practice. Jones & Bartlett Pub. (1993)
[3] Roberts, V.C.: Photoplethysmography – Fundamental aspects of the optical properties of blood in motion. Trans. Inst. Meas. Control 4, 101–106 (1982)
[4] Roggan, A., Friebel, M., Dörschel, K., Hahn, A., Müller, G.: Optical properties of circulating human blood in the wavelength range 400-2500 nm. J. Biomed. Opt. 4, 36–46 (1999)
[5] Prahl, S.A., Keijzer, M., Jacques, S.L., Welch, A.J.: A Monte Carlo model of light propagation in tissue. In: Proc. SPIE IS, 6th edn., vol. 5 (1989)
[6] Prahl, S.A.: Inverse adding-doubling program. Oregon Medical Laser Center, St. Vincent Hospital (2011)
[7] Kamal, A.A.R., Hatness, J.B., Irving, G., Means, A.J.: Skin photoplethysmography – a review. Comput. Methods Programs Biomed. 28, 257–269 (1989)
[8] Schmidt, H.M., Lanz, U.: Chirurgische Anatomie der Hand. Stuttgart, Hippokrates, Verlag (1992)
[9] Niemz, M.H.: Laser-Tissue Interactions – Fundamentals and Applications. IEEE Journal of Quantum Electronics QE-32, 1717–1722 (1996)
[10] Kraitl, J.: Die nichtinvasive Bestimmung der Hämoglobinkonzentration im Blut mittels Pulsphotometrie. MBV Verlag, Berlin (2007) ISBN 3-86664-361-6
[11] Wang, L., Jacques, S.L., Zheng, L.: MCML-Monte Carlo modeling of light transport in multi-layered tissues. Computer Methods and Programs in Biomedicine 47, 131–146 (1995)
[12] Veach, E., Guibas, L.J.: Robust monte carlo methods for light transport simulation. Stanford University, Stanford (1998)
[13] Sobol, I.M.: A Primer for the Monte Carlo Method. CRC Press, Boca Raton (1994)
[14] Born, M., Wolf: Principles of Optics: Electromagnetic Theory of Propagation, Interference and Diffraction of Light, 6th (corrected) (edn.) Pergamon Press, New York (1986)
[15] Yaroslavsky, A.N., Yaroslavsky, I.V., Goldbach, T., Schwarzmaier, H.J.: The optical properties of blood in the near infrared spectral range, in Optical Diagnostics of Living Cells and biofluids. In: Proc. SPIE, Int. Soc. Opt. Eng., vol. 2678, p. 314 (1996)
[16] Tuchin, V.: Tissue Optics - Light Scattering Methods and Instruments for Medical Diagnosis, 2nd edn., pp. 145–191. SPIE (2007)
[17] Bashkatov, A.N., Genina, É.A., Kochubey, V.I., Tuchin, V.V.: Optical Properties of the Subcutaneous Adipose Tissue in the Spectral Range 400 – 2500 nm. Text 99, 868–874 (2005)

[18] Troy, T.L., Thennadil, S.N.: Optical properties of human skin in the near infrared wavelength range of 1000 to 2200 nm. J. Biomed. Opt. 6, 167 (2001)
[19] Weininger, S.A.: Prototype device for standardized calibration of pulse oximeters II. Journal of Clinical Monitoring and Computing (2002)
[20] Firbank, M., Oda, M., Delpy, D.T.: An improved design for a stable and reproducible phantom material for use in near-infrared spectroscopy and imaging. Physics in Medicine and Biology 40, 955–961 (1995)
[21] Lualdi, M., Colombo, A., Farina, B., Tomatis, S., Marchesini, R.: A phantom with tissue-like optical properties in the visible and near infrared for use in photomedicine. Lasers Surg. Med. 28, 237–243 (2001) doi: 10.1002/lsm.1044
[22] Firbank, M.: A design for a stable and reproducible phantom for use in near infrared imaging and spectroscopy. Physics in Medicine and Biology 38, 847–853 (1993)
[23] Koh, P.H., Elwell, C.E., Delpy, D.T.: Development of a dynamic test phantom for optical topography. Adv. Exp. Med. Biol. 645, 141–146 (2009)
[24] Roggan, A., Friebel., M., et al.: Optical Properties of circulating human blood. BIOS Europe (1997)
[25] Kraitl, J.: Optisches Monitoring für die in-vitro –Messung der Hämoglobin Konzentration und der Sauerstoffsättigung. In: BMT 2006, Zürich, Schweiz (2006)
[26] Fricke, D., Koroll, H., Kraitl, J., Ewald, H.: Blood flow model for noninvasive diagnostics. In: Proceedings of IEEE GCC Conferenc and Exhibition, Dubai, UAE, pp. S.343–S.346 (2011) ISBN 978-1-62284-118-2
[27] Kraitl, J., Ewald, H., Gehring, H.: An optical device to measure blood components by a photoplethysmographic method. J. Opt. A.: Pure Appl. Opt. 7, 318–324 (2005)
[28] Kraitl, J., Timm, U., Lewis, E., Ewald, H.: Optical sensor technology for a noninvasive continuous monitoring of blood components. In: BIOS, SPIE Photonics West, San Francisco, CA, USA (2006)